Plant Genet Transgenics 2012 3(1):1-13

Journal of Plant Genetics and Transgenetics

www.academyjournals.net

ISSN 2146 0949

Original Article

Characterization of Poplar *ZIP* Family Members *ZIP1.2* and *ZNT1*

Joshua Pope ADAMS[1*], Ardeshir ADELI[2], Chuan-Yu HSU[3], Richard L. HARKESS[4], Grier P. PAGE[5], Claude W. de PAMPHILIS[6], Yuannian JIAO[6], Emily B. SCHULTZ[3], Cetin YUCEER[3]

[1] *School of Forest Resources, University of Arkansas-Monticello, Monticello, AR 71656, USA;*
[2] *USDA-ARS, 810 Highway 12 East, Mississippi State, MS, 39762, USA;*
[3] *Department of Forestry, Mississippi State University, Mississippi State, MS 39762, USA;*
[4] *Department. of Plant and Soil Science, Mississippi State University, 142A Dorman Hall, Box 9555, Mississippi State, MS 39762, USA*;
[5] *RTI International, Atlanta, GA 30341-5533, USA;*
[6] *Department of Biology, Pennsylvania State University, University Park, PA 16802, USA*

Received: 19.03.2012 ***Accepted: 13.04.2012*** ***Published: 02.05.2012***

Abstract

Regulation of a heavy metal such as zinc (Zn) throughout a plant has been attributed to the Zn transporter gene *ZNT1* and other members of the larger ZIP transporter family. However, genes have not been characterized in a high-biomass, perennial, woody species, such as poplar (*Populus trichocarpa*). The poplar genome was searched for ZIP transporter members and analyzed via a phylogenetic analysis. Afterwards, two of these genes were selected for further characterization via transcriptional analysis. Poplar appears to contain 13 genes with sequence orthology to ZIP family members. Of these 13 genes, only one gene appears to be a close ortholog to the TcZNT1 gene in the hyperaccumulating *Thlaspi caerulescens* (syn. *Noccaea caerulescens*). Transcript abundance of this poplar ortholog, *PtZNT1,* and another ZIP poplar member, *PtZIP1.2,* generally decreased in stem and root tissue, respectively, as levels of Zn increase in poplar. Furthermore, *PtZNT1* promoter abundance does not localize to a specific tissue nor have the overall promoter abundance of *TcZNT1* which localizes in vascular tissue. *PtZNT1* promoter abundance is stable and active across tissues but at an overall lower level than the hyperaccumulator. These characterizations of ZIP members in poplar may indicate a specifically evolved coordination of tissue specific Zn transporters for regulation of nutrients.

Key words: Poplar, Zinc, ZIP Gene Family, ZNT1, Heavy-Metal, Hyperaccumulator

[*]*Corresponding Author: J. P.Adams, e-mail: AdamsJ@uamont.edu Phone: +1-870-460-1348*

INTRODUCTION

Plants use a variety of transport proteins to regulate interaction with heavy metals, ensuring adequate availability without the toxicity incurred from excesses. One essential heavy metal required for many plant processes is zinc (Zn). However, a critical balance maintained in which adequate Zn is absorbed and transported throughout the plant, while excesses that can cause damage due to competition with other essential elements (e.g., iron [Fe], copper [Cu], and calcium [Ca]) are prevented (Clemens et al., 1999; Hartwig et al., 2002; Michaelis et al., 1986).

Species have evolved various strategies to maintain this delicate balance of heavy metal regulation. Even within a

single plant family (e.g., Brassicaceae) there are extreme plant-heavy metal interaction phenotypes. At one extreme, low metal accumulation phenotypes are present in pakchoi (*Brassica chinensis*) and Chinese cabbage (*Brassica rapa*) with less than 200 mg kg^{-1} Zn acting as a lethal threshold (Long et al., 2003). At the other extreme are the hyperaccumulators *Thlaspi caerulescens* (syn. *Noccaea caerulescens*) and *Arabidopsis halleri* which can withstand up 30,000 mg kg^{-1} Zn. Interestingly, all these species have a similar group of heavy metal transport genes which affect the plants interaction with Zn and other essential metals by specifically controlling root absorption, transport via vascular tissue, and use or storage in areas of active meristematic activity. The several characterized transport proteins include the zinc transporter (ZNT), heavy metal ATPase (HMA), and iron regulated transporter (IRT) (Bernard et al., 2004; Grotz et al., 1998; Mills et al., 2003).

Both ZNT and IRT, members of a much larger Zrt (Zinc Regulated Transporter), Irt (Iron Regulated Transporter)-like Protein (ZIP) family, play essential roles in the regulation of Zn, Fe, and even cadmium (Cd) uptake among a wide variety of species (Chiang et al., 2006; Eng et al., 1998; Guerinot, 2000; Ramesh et al., 2004; Yang et al., 2009). Also, genes from this *ZIP* family, specifically *ZNT1*, have been associated with the hyperaccumulating phenotypes such as that found in *T. caerulescens.* However, characterization of these specific genes affecting plant-heavy metal interactions has been mostly relegated to small, annual species which are not adequate for large scale remediation (Pence et al., 2000).

High-biomass, perennial species such as poplar (*Populus trichocarpa*) could potentially be used for bioremediation, but only a few studies in such plants of metallothioneins, glutathione, cation diffusion facilitator, and heavy metal ATPase (Adams et al., 2011; Blaudez et al., 2003; Di Baccio et al., 2005; Kohler et al., 2004) have been conducted. The goal of this study was to characterize *ZIP* family genes in poplar via three objectives. First, members of the gene family in poplar were identified; secondly, transcript abundance of two key members was explored. Finally, localization of poplar *ZNT* and *T. caerulescens ZNT* promoter abundance was compared in an *Arabidopsis thaliana* host. Knowledge gained from these three objectives aids in elucidating the *ZIP* family in poplar and characterizing the mechanisms controlling its Zn-interaction phenotype.

MATERIAL AND METHODS

Identification of poplar *ZIP* members and an ortholog to *TcZNT1*

Two phylogenetic analyses were conducted to (1) place poplar *ZIP* family members in context with family members from other species and (2) identify a poplar ortholog to *T. caerulescens ZNT1* (i.e., *TcZNT1*). In the phylogenetic analyses, possible poplar *ZIP* members were retrieved from keyword searches, eudicot gene cluster searches, sequence blasts (i.e., blastp) of the NCBI database (www.ncbi.nlm.nih.gov), and the Phytozome v 5.0 database (www.phytozome.net/poplar.php) which includes the *P. trichocarpa* genome v 2.2. Potential orthologs from an array of other species, both dicot and monocot, were included. Genes included were from *A. thaliana* (13 genes) and poplar (13 genes) *ZIP* cluster members from the Phytozome v 5.0 database (cluster 23249139). Also included were eight monocot *ZIP* genes from rice (*Oryza sativa*) and sorghum (*Sorghum bicolor*) as well as *TcZNT1*. Transcript sequences were collected, translated into amino acid sequences, and aligned with the protein alignment software MUSCLE using default parameters (Edgar, 2004). The original coding sequences were then forced onto their respective aligned amino acid sequence using a Perl script. Maximum likelihood (ML) analysis was conducted with RAxML version 7.2.1 (Stamatakis, 2006; Stamatakis et al., 2005) using a rapid bootstrap analysis (100 replications) with the General Time Reversible model of DNA sequence evolution with the gamma-distributed rate heterogeneity (GTRGAMMA). Potential structural orthology of *ZIP* family members was analyzed by comparing each amino acid sequence's predicted transmembrane helices calculated with the prediction algorithm TMMTOP (Tusnady and Simon, 1998).

A second phylogenetic analysis was conducted to more precisely identify the specific poplar ortholog(s) to *TcZNT1*. This analysis used only *A. thaliana* (13 genes) and poplar (13 genes) *ZIP* cluster members from the Phytozome v 5.0 database. Similar to the previous analysis, eight monocots *ZIP* genes from rice (*Oryza sativa*) and sorghum (*Sorghum bicolor*) as well as *TcZNT1* were included. The previous procedures for alignment and tree building were used.

Zn challenge assay and effect on *PtZNT1* and *PtZIP1.2*

Poplar plants were propagated for metal assays. Stem segments (approximately 15-20 cm) were harvested from field grown *P. trichocarpa* cv. Nisqualy in early spring, dipped in Hormex© rooting powder #16 (Hollywood, CA), planted in moist soil, and grown in a greenhouse from early March to May. The greenhouse provided for temperature control through limiting temperature highs to no more than 32 °C; however, there was no humidity control or supplementary lighting. A water misting system was used that misted every 5 min for 30s at a rate of 15 L h^{-1}. Each plant was transplanted into sterile sand in a 12.25 cm diameter pot with an attached water-catching basin. Plants were supplemented with Hoagland's nutrient solution every two days for eight days

and then randomly assigned to three metal treatments and two harvesting times, with each treatment-by-harvest time combination containing eight replications. Three metal treatments were used containing no additional Zn (unmodified Hoagland's solution with 1μM $ZnSO_4$ [control]), 10μM, and 1mM $ZnSO_4$. The harvest times were 24h and 48h after application of Zn treatments. At harvest, the plants were washed, and leaves, stems, and roots were frozen separately in liquid nitrogen, and stored in a -80˚C freezer.

RNA was extracted from these tissues using a hot borate RNA extraction method (Wan and Wilkins, 1994) followed by on-column DNase I treatment (Promega; Madison, WI) and RNA cleanup via the RNeasy Plant Mini Kit (Qiagen; Valencia, CA). One micro-gram of RNA was reverse-transcribed using M-MLV reverse transcriptase (Promega; Madison, WI). *PtZNT1* (*POPTR_0018s05190.1*) transcription abundance differences across tissue, day, and metal treatment were analyzed via real-time quantitative PCR (qPCR) using TaqMan probe and TaqMan master mix (Applied Biosystems, Foster City, CA). Another gene, *POPTR_0008s08260.1* (*PtZIP1.2)*, identified in the phylogenetic analysis as a close *ZIP1* ortholog, was analyzed for transcriptional abundance via qPCR using Power Sybr-Green master mix (Applied Biosystems; Foster City, CA). This second gene was selected to broaden the expression study with a gene located distantly on the phylogenetic tree from the clade containing *TcZNT1*. *Ubiquitin* (*UBQ*) transcript amplification was used as a standard for both qPCR analyses and was assayed using both protocols and appropriate primers (Infante et al., 2008). For the Power Sybr-Green reactions, all primers (Appendix S1) in qPCR reactions were verified for specificity via ABI Prism dissociation curve analysis software and PCR products were separated by electrophoresis on a 1% agarose gel. Standard curves for Sybr-Green qPCR were constructed using serial dilutions of cDNA.

For both *PtZNT1* and *PtZIP1.2* transcripts, amplification reactions were performed using an ABI 7500 Fast Real-Time PCR System (Applied Biosystems; Foster City, CA) for relative transcript quantification. Each reaction was independently repeated at least three times. Transcripts analyzed with both qPCR reactions used the cycle threshold amplification points (C_t values) relative to *UBQ* C_t values from each prospective qPCR protocol resulting in a ratio. Ratios for both investigated transcripts were log10 transformed and analyzed by tissue with a mixed-effect general linear model in which there was a fixed metal effect, a fixed day co-variant effect, and a random biological (plant) effect.

ZNT promoter isolation and abundance assays

PtZNT1 and *TcZNT1* promoters were isolated, cloned, and studied for abundance and localization. Primers were first designed for isolation of an approximate 2.0 kilobase segment upstream of the *PtZNT1* start codon in *P. trichocarpa* (Appendix S1). Genomic DNA was extracted from leaf tissues using the DNeasy Plant Mini Kit (Qiagen; Valencia, CA). Genomic-PCR was conducted using a three-step (94 °C-30s, 55 °C-60s, and 72 °C-120s) 30 cycle program using ex-*Taq* polymerase (Takara Bio Inc.; Shiga, Japan), buffer, and select primers. The amplicon was cloned into the pGEM-T Easy vector (Promega; Madison, WI) and sequenced with CEQ 8000 Genetic Analysis System (Beckman-Coulter; Brea, CA). Restriction sites were added with a second PCR reaction using the cloned promoter segment as the template, primer pairs with added restriction sites, and *Pfu* DNA-polymerase (Stratagene; La Jolla, CA). The amplified sequence was cloned into the pGEM-T Easy vector and re-sequenced to ensure no errors.

The *TcZNT* promoter was isolated by first conducting genome walking because the genome of *T. caerulescens* is unresolved. First, *T. caerulescens* DNA was isolated from leaf tissue using the DNeasy Plant Mini Kit (Qiagen; Valencia, CA) and digested with *DraI* for library creation. Adapters provided in the BD GenomeWalker Universal Kit (BD Biosciences, San Jose, CA) were added to the digested fragments and PCR was used to amplify the segment up-stream of *TcZNT1* start codon using a universal primer for the adapter and a primer designed for the *TcZNT1* gene (Appendix S1). The resulting amplicon was purified, cloned into pGEM-T Easy, and sequenced. This sequence was aligned with the known *TcZNT1* gene sequence resulting in a 781-bp promoter sequence and 1214-bp overlapping region. This process was repeated to extend the sequence coverage using a new primer (TcZNT-prom1) and a *PvuII* digestion library. The 1385-bp amplicon, with a 290-bp overlapping region with the previous amplicon, was sequenced. After this two-step process, a known 1556-bp sequence upstream of *TcZNT1* was isolated using PCR with ex-*Taq* polymerase, cloned into pGEM-T Easy, and re-sequenced.

Both promoters were cloned into the binary vector pBI121 (Clontech; Mountain View, CA) replacing the CaMV 35S constitutive promoter upstream of the beta-glucuronidase (GUS) reporter gene. Each construct (Pro_{PtZNT1}*:GUS* and Pro_{TcZNT1}*:GUS*) was transformed into *Agrobacterium tumefaciens* strain C58, and subsequently to *A. thaliana* using a floral-dip transformation protocol (Clough, 2005). Seeds from successive generations of *A. thaliana* lines were screened on agar plates with one-half Murashiga and Skoog (MS) media with added Kanamycin (50 mg ml^{-1}). The fifth-generation of *A. thaliana* lines from both Pro_{PtZNT1}*:GUS* and Pro_{TcZNT1}*:GUS* constructs were further screened for positive gene insertion using PCR confirmation. Subsequently, positive lines were planted, harvested one week after germination, and assayed via a non-quantitative histochemical

GUS assay. Three average lines, based on average GUS expression during PCR confirmation, from both constructs were selected and used in slide preparations and viewing under a light microscope. Each of the selected lines was planted in sterile, inert sand, grown for two weeks, and harvested. Tissues were incubated overnight at 37 ºC in GUS staining solution and washed till tissue cleared using a 50% ethanol solution. Whole plant samples were viewed under a light microscope. Also, leaf and root samples were fixed in half-strength Karnovsky's fixative (2% paraformaldehyde and 2.5% glutaraldehyde) with phosphate buffer (0.1 M, pH 7.2). Samples were then rinsed in distilled water and dehydrated in a graded ethanol series. Leaf and root samples were infiltrated and embedded in Paraplast Plus (Oxford Labware, St. Louis, MO) using CitriSolve (Fisher Scientific, Houston, TX) as a transitional fluid. Serial 8 micron sections were cut with an American Optical 820 rotary microtome (Fisher Scientific, Houston, TX), stained with saffranin and fast green, and placed on glass slides for light microscope viewing.

Promoter abundance via GUS gene expression of the Pro_{PtZNT1}*:GUS* and Pro_{TcZNT1}*:GUS* constructs was studied via qPCR. Leaf and root tissues were harvested from the three selected *A. thaliana* lines of each construct grown for 2 months in sterile sand. These plants were grown indoors under 25 °C with artificial lighting of ~60 µmoles $s^{-1}m^{-2}$ under 8/16 h (night/day) day-length. Using previous procedures, tissues were frozen and RNA was extracted. After cDNA was synthesized, transcriptional abundance of the GUS gene was assayed for relative transcript quantification via qPCR with two GUS primers using previous Sybr-Green protocol (Appendix S1). Log10 ratios of GUS transcript abundance relative to the amount of *UBQ* transcript abundance were analyzed with a Student's t-test. First, expression differences were tested between the overall Pro_{PtZNT1}*:GUS* construct and Pro_{TcZNT1}*:GUS* constructs. Then, GUS transcript abundance in roots and stems (stem and leaves) were compared between constructs. Finally, within each construct, GUS transcript abundance between the two tissues was compared.

RESULTS

Poplar contains several *ZIP* gene family members

The poplar ortholog to *TcZNT1* was identified in both phylogenetic trees as *PtZIP(5) [POPTR 0018s05190.1]* (Figure 1). These trees mirrored generally established species trees in which the core eudicot group of *ZNT* orthologs is spatially distant from both the monocot genes. Analysis of poplar genes in context of the *ZIP* gene family of *A. thaliana* supports *PtZIP(5) [POPTR 0018s05190.1]* as the closest poplar ortholog to *TcZNT1* (Figure 1). While poplar contained 13 genes in both phylogenetic trees, this one poplar gene was conspicuously closer to the known *TcZNT1* and *TjZNT1* orthologs and was the best blast hit when blasting *TcZNT1* into the poplar genome with 69.4% sequence similarity. Structural similarity within the tree, as predicted from transmembrane helix predictions, is very strong across species. The majority of these genes, including the poplar gene closest to known *ZNT1* genes, have translated proteins predicted to have eight helices (Appendix S2). Because of the apparent close othology between *TcZNT1* and *PtZIP(5),* it will henceforth be termed *PtZNT1*.

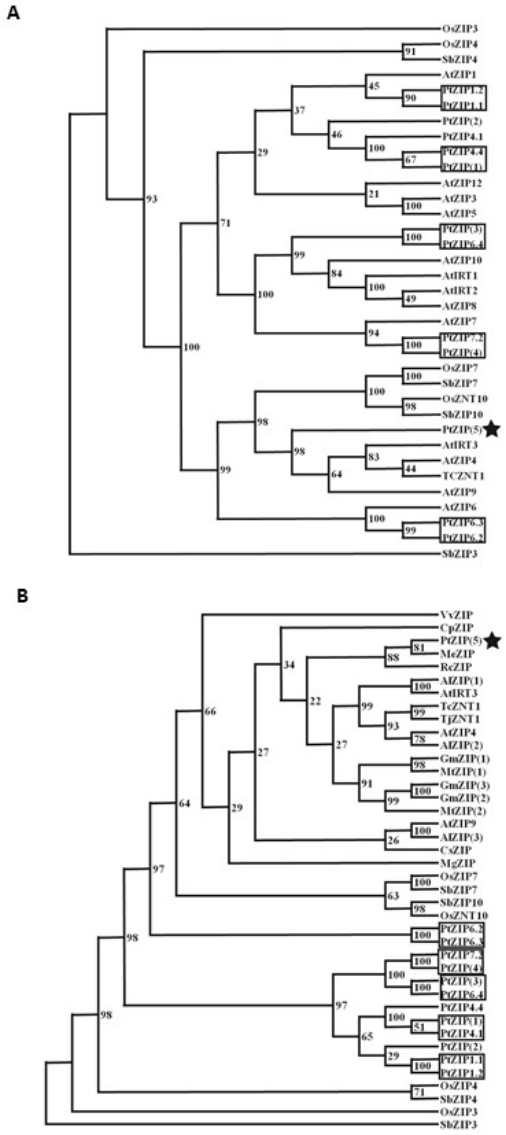

Figure 1 Maximum likelihood phylogenetic trees of (a) the broad *ZIP* family of genes from *A. thaliana* and poplar and (b) close orthologs of *TcZNT1* across many plant species. Gene names are listed based on annotations from each species respective database, unless there was no specific annotation; in which case, they are listed by a random number in parentheses. Bootstrap percentages (n=100) greater than 50% are located at nodes. Each tree contains a gene from the hyper-accumulator *Thlaspi caerulescens* annotated as *ZNT1* (i.e., *TcZNT1*). The closest poplar homolog to *TcZNT1* is indicated by a solid black star and is referred throughout the text as *PtZNT1*. Accession numbers corresponding to the gene names are located in Appendix S2. Species include: Pt-*Populus trichocarpa,* Ah-*Arabidopsis halleri*, Al-*Arabidopsis lyrata*, At-*A. thaliana*, Tj-*Thlaspi japonicum*, Tc- *Thlaspi caerulescens*, Bj- *Brassica juncea*, Bn-*Brasscia napus*, Cp-*Carica papaya*, Rc-*Ricinus comunis*, Me- *Manihot esculenta*, Vv-*Vitis vinifera*, Cs-*Cucumis sativus*, Sr-*Sesbania rostrata*, Gm- *Glycine max*, Mg-*Mimulus guttatus*, Nt-*Nicotiana tabacum*, Ng-*Nicotiana glauca*, and two monocots Os-*Oryza sativa* and Sb-*Sorghum bicolor. P. trichocarpa* gene pairs enclosed by a black box indicate that they are identified members of the Salicoid gene duplication event.

PtZNT1 and *PtZIP1.2* expression across the metal gradient

A previous study found significant Zn accumulation changes in poplar roots, but not in stems or leaves, after only 24 hours of exposure using the same metal treatments used in this study (Adams et al., 2011). *PtZNT1* expression in leaf tissues was not significantly (p=0.26) altered across metal concentrations (Appendix S3). However, expression abundance varied significantly between stems and roots, where stem expression was about 73% higher than root expression. *PtZIP1.2* expression had an opposite trend in roots and stems compared to *PtZNT1* roots and stems, with an overall 65% higher transcript abundance average in roots than in stems across treatments. Within the stem tissue both *PtZNT1* and *PtZIP1.2* expression significantly varied across the Zn gradient [p=0.006 and <0.001 respectively (Figure 2a, b respectively)]. There was also a significant co-variant time effect for *PtZIP1.2* (p=0.01) which had 4.28-fold greater abundance 24h after Zn treatment compared with 48h. On the other hand, *PtZNT1* was stable across the co-variant time effect (p=0.77). A distinct trend was seen in transcription abundance across metal treatment in stem tissue for *PtZIP1.2* which had a significant 56% decrease from the 1µM Zn treatment to the 1mM Zn treatment. Although significant, the *PtZNT1* gradient trend was centric, where both the 1mM and 1µM treatments were significantly different from the 10µM treatment but not significant from each other. *PtZNT1* in roots was significantly and negatively affected by the 1mM concentration of Zn [p=0.02] decreasing 46% between the 10µM and 1mM treatments (Figure 2c), and similar to its expression in stem tissue, *PtZNT1* was stably expressed across time (p=0.34). *PtZIP1.2* expression in roots was only significantly different (p=0.008) in the 10µM Zn treatment and a trend could not be defined (Figure 2d). Like in stem tissues however, *PtZIP1.2* transcript abundance was significantly affected (p<0.01) by the day covariant in which there was 1.5-fold greater transcript abundance after 24h compared to 48h.

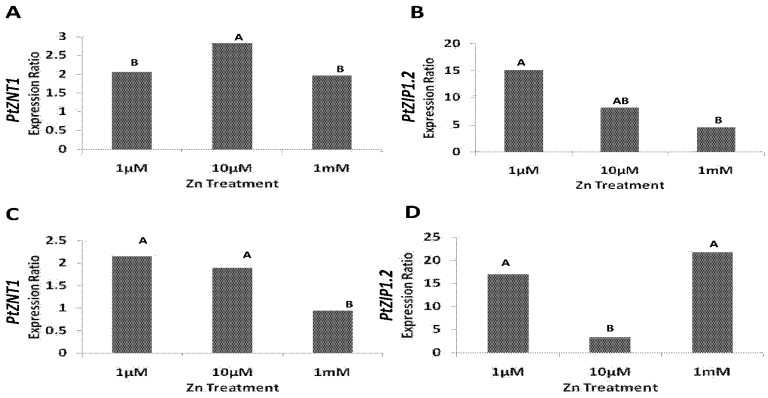

Figure 2 Effect of Zn exposure (1µM, 10µM, and 1mM) on the ratio of *PtZNT1* (a) stem and (c) root and *PtZIP1.2* (b) stem and (d) root expression to *UBQ* expression. Letters in each section represent Fisher's Protected LSD mean separation where differing letters represent significantly different means at the 0.05 level.

Pro_{PtZNT1}:*GUS* and Pro_{TcZNT1}:*GUS* abundance localizes differently in tissues

GUS abundance from both Pro_{PtZNT1}:*GUS* and Pro_{TcZNT1}:*GUS* constructs was evident in *A. thaliana* plants following the staining procedure. While this was not a quantitative procedure, there was a clear difference between promoter localization between the two constructs. The poplar construct (Pro_{PtZNT1}:*GUS*) had clear GUS presence across all tissues [i.e., roots, stems, and leaves (Figure 3a)]. *T.*

caerulescens promoter localized only in the root and stem vascular tissue and in the leaf midrib and veins (Figure 3b).

Upon closer inspection under a light microscope, GUS abundance from *Pro$_{PtZNT1}$:GUS* was observed throughout all leaf cells within the epidermis including the palisade mesophyll and spongy mesophyll (Figure 3c). The apparent lack of *Pro$_{TcZNT1}$:GUS* localization in leaves is seen in a tangential view of the leaf where GUS abundance, like *Pro$_{PtZNT1}$:GUS* construct abundance, is not observed within the epidermis, but in the mesophyll (Figure 3d). Unlike the *Pro$_{PtZNT1}$:GUS* construct, the expression is not constitutive throughout the mesophyll cells. While there is leaf expression, this sporadic expression seems to be localized only in the mesophyll and leaf vascular bundle cells (Figure 3b,d).

While GUS visualization showed localized differences between tissues, quantification of transcript abundance via qPCR analysis demonstrated that expression in roots was only marginally greater (not significant) than leaves in both constructs. GUS transcriptional abundance in leaf tissues was approximately 67% (p=0.42) and 74% (p=0.47) the abundance of roots in *Pro$_{TcZNT1}$:GUS* and *Pro$_{PtZNT1}$:GUS* constructs respectively (Appendix S4). There was a difference between the overall construct ratios (p=0.0034) with the *Pro$_{TcZNT1}$:GUS* construct expressed 2.65 times greater than the *Pro$_{PtZNT1}$:GUS* construct. Also, there were differences between the two constructs in both leaf (p=0.05) and root (p=0.04) expression (Figure 3e).

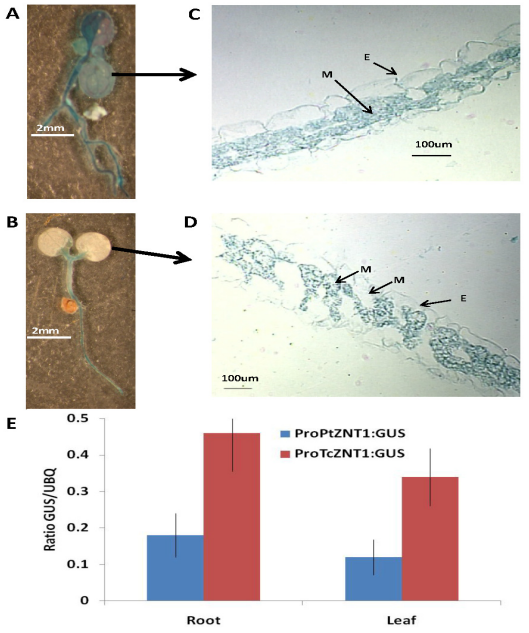

Figure 3 GUS abundance (blue coloration) throughout the whole plant for (a) *Pro$_{PtZNT1}$:GUS* and (b) *Pro$_{TcZNT1}$:GUS* constructs. Major color differences observed in leaves were further investigated with visualization of leaf cross-sections from the (c) *Pro$_{PtZNT1}$:GUS* and (d) *Pro$_{TcZNT1}$:GUS* constructs. (e) The ratio of *Pro$_{PtZNT1}$:GUS* and *Pro$_{TcZNT1}$:GUS* expression to *UBQ* expression from root and leaf tissues were compared. Error bars represent standard error of the mean. M = Mesophyll cells; E= Epidermis.

DISCUSSION

The *ZIP* gene family is a large and ancient gene family systemic to bacteria, plants, and animals (Balesaria and Hogstrand, 2006). The *A. thaliana* genome alone contains at least 15 members and is responsible for much of the Zn and Fe cellular uptake in plants (Chen et al., 2008; Guerinot, 2000; Wu et al., 2009). Some individual genes from this family such as *IRT1* and *ZNT1* have also been linked to hyperaccumulation phenotypes (Lombi et al., 2002; Pence et al., 2000). Thus, potential use of high-biomass woody species for remediation requires an understanding of this gene family. Identification and characterization of family members in the tree species *P. trichocarpa* is a vital first step toward this goal and to the overall understanding of heavy metal plant interactions.

The poplar *ZIP* family had 13 closely related members and precisely matched the number of *ZIP* family members in *A. thaliana* in the same cluster (all were members of the Phytozome cluster 23249139). Granted, there are more *ZIP* members that are more distant from the core Eudicot group in the study (e.g., Mäser et al.(2001) report a total of 15 *AtZIP* genes) and these are more diverse *PtZIP* members from poplar that are outside this core Eudicot group (Migeon et al., 2010). The poplar *ZIP* family members that were included indicated that at least five arose from the Salicoid whole genome duplication after divergence from *A. thaliana* (Tuskan et al., 2006). However, there is a lack of gene diversity compared to *A. thaliana* in which all 13 *AtZIP* members are annotated as independent *ZIP* transporters (e.g., *ZIP1, IRT3, ZIP4, ZIP5, ZIP7, and ZIP12*). In poplar, *ZIP* transporters form sub-clusters (e.g., *PtZIP(1), PtZIP4.4, PtZIP4.1, and PtZIP(2)*) as supported by a recent tree of *ZIP* poplar genes (Migeon et al., 2010). The *ZIP* family component in poplar also has a general conservation of predicted transmembrane loops in which most have 8-9 helices typical of the *ZIP* gene family (Eng et al., 1998; Gaither and Eide, 2001; Moreau et al., 2002). Interestingly, the section of the tree containing *TcZNT1* is the most uniform in regards to these predicted helices but represented species with Zn sensitive and Zn hyperaccumulating phenotypes. Because of the similarities in coding sequence and predicted protein structure, transcriptional abundance differences among species may play a role in determining metal phenotype.

From the *ZIP* gene family we chose close orthologs to *TcZNT* and *AtZIP1* (i.e., *PtZNT1* and *PtZIP1.2,* respectively) since these are important to zinc homeostasis. Differences in localization and transcriptional patterns were observed in this study (i.e., expression patterns of *PtZIP1.2* and *PtZNT1*) and within other species (Devergnas et al., 2004; van de Mortel et al., 2006; Yang et al., 2009); however, functionality differences among poplar *ZIP* family members is unclear (Lopez-Millan et al., 2004; Wu et al., 2009). Indeed, genome duplications have resulted in nearly half of the entire poplar ZIP family (i.e., *PtZIP1.2, PtZIP1.1, PtZIP(2), PtZIP4.1, PtZIP4.4,* and *PtZIP(1)*) clustering closely to *AtZIP1* which may indicate that ZIP1-like genes play important roles in poplar. In this study, *ZIP1.2* in poplar stem tissue, similar to orthologs *AtZIP1* (*A. thaliana*), *AhZIP1* (*A. halleri*), *MtZIP1* (*Medicago truncatula*) (Becher et al., 2004; Lopez-Millan et al., 2004; Ramesh et al., 2004), is up-regulated under adequate Zn and is down-regulated under Zn excesses (Figure 2b). Evolving on sites subject to recurring flooding and drought stress that can cause fluctuations in available nutrients (Adair and Binkley, 2002; Rood et al., 2003) may have favored increased presence of these *ZIP1*-like genes allowing poplar to maintain needed metal concentrations in depletion conditions.

Unlike the multiple *ZIP1*-like gene paralogs, poplar contains only one gene closely related to *TcZNT1*. *Arabidopsis thaliana,* on the other hand, has two to three genes in the same clade, where *AtZIP4* is the closest ortholog to *TcZNT1* (Assuncao et al., 2001; Chen et al., 2008; Pence et al., 2000; Wu et al., 2009) and additional genes *AtIRT3* and *AtZIP9* were also spatially close (Figure 1a). Since there was not a simple pairing of poplar genes to *A. thaliana* genes and this study has subtle differences from a recent attempt to comprehensively classify metal transporters in poplar (Assuncao et al., 2001; Migeon et al., 2010; Pence et al., 2000), *POPTR 0018s05190.1* [*PtZIP(5)* in Figure 1], we provisionally use the name *PtZNT1* since its closest ortholog, in both trees, is *TcZNT1*.

The expression of two poplar genes in the *ZIP* family is different than that seen in hyperaccumulator phenotypes. *T. caerulescens* controls its Zn intake in part through localized expression in vascular tissues and reported constitutive or increasing expression across Zn availability (Kupper and Kochian, 2010; Pence et al., 2000; van de Mortel et al., 2006; Wu et al., 2009). Alternatively, the non-hyperaccumulator *T. arvense* and *A. thaliana* both down-regulate their *ZNT1* orthologs as metal concentrations increase which is similar to trends seen in the other *ZIP* members (Grotz et al., 1998; Kawachi et al., 2009; Milner and Kochian, 2008). Likewise in poplar roots, a drastic decline in *PtZNT1* expression is evident between the 1mM Zn concentration and the lower Zn treatment concentrations of 10µM and 1µM Zn (Figure 2c). This poplar gene response occurs very rapidly (24h) after the addition of metals, indicating poplar's tight control of its metal accumulation through *PtZNT1* expression in roots and a coordinated response in the stem with decline of *PtZIP1.2* expression.

Promoter activities of poplar and *T. caerulescens ZNT1* genes are different. When *ZNT1* was first characterized in *T. caerulescens,* it was determined to be highly expressed in root tissue and to a lesser extent leaf tissue (Pence et al., 2000). This is similar to the expression pattern observed in another Zn transporter, *TcHMA4*, often related to hyperaccumulation that is primarily localized in roots, helping to load excess Zn into the xylem for long distance transport (Papoyan and Kochian, 2004). Since *T. caerulescens* hyperaccumulation phenotype has been specifically linked to roots (de Guimaraes et al., 2009), localization of Zn transporters may be partly responsible for the hyperaccumulation phenotype (Grispen et al., 2011). However, qPCR transcript analysis shows no statistical difference between leaf and root tissue abundance in either construct. A difference in localization of *TcZNT1* is apparent in leaf tissue in which abundance is sporadic through the mesophyll cells and in the leaf vascular bundle (Figure 3d) confirming the quantitative *in situ* hybridization results by Kupper et al. (2007) which showed expression in photosynthetic mesophyll and guard cells. This points toward some reliance on *TcZNT1* for Zn regulation under moderate (i.e., neither deficient nor surplus) Zn growing conditions, and a modulation in the promoter that has caused hyperabundance leading to increased transport via vascular tissues. In contrast, the poplar *ZNT* gene has a promoter that does not directly localize to specific photosynthetic areas including epidermal cells similar to the expression patterns of *TcZNT5* (Kupper and Kochian, 2010). Also, it is expressed at much lower levels than the hyperaccumulator, indicating that this transporter is used for more general Zn supply regulation.

Poplar has adapted to address ecological pressures; mainly, large fluctuations of water and available nutrients including Zn. The two poplar genes studied here play alternate roles in maintaining the Zn balance resulting in a coordinated tissue specific response. As Zn concentrations rise, *PtZNT1* expression decreases in roots stifling further intake; while *PtZIP1.2* expression levels are generally maintained. This may lead to increased expulsion of Zn from cells into the apoplast, decreasing cellular concentrations below toxic levels (Lee et al., 2003). Similar modulations occur in a large array of non-hyperaccumulators such as *T. arvense* (Hammond et al., 2006) and even highly diverged human epithelial cells (Devergnas et al., 2004). While poplar has multiplied and altered its contingent of *ZIP* genes, the underlying ancestral mechanisms for regulating Zn have been maintained.

ACKNOWLEDGEMENTS

We thank all of our student workers that have assisted at various times through the course of this project, most notably L. Vandervelde, M. Monroe, and J. Ellis. Also, A. Lawrence provided invaluable help with slide preparation, A. Karsi assisted with microscope use, and S. Ebbs (Southern Illinois University) for *T. caerulescens* seeds. We also thank M. Aarts (Wageningen University) for providing a critique of this paper. This paper was developed under a STAR Research Assistance Agreement No. FP916894 awarded by the Environmental Protection Agency. It has not been formally reviewed by the EPA. The views expressed in this paper are solely the view of the authors and the EPA does not endorse any products or commercial services mentioned in this paper. This manuscript is #FO-401 from the Forest and Wildlife Research Center, Mississippi State University.

REFERENCES

Adair EC Binkley D, 2002. Co-limitation of first year Fremont cottonwood seedlings by nitrogen and water. Wetlands 22: 425-429

Adams JP, Adeli A, Hsu CY, Harkess RL, Page GP, dePamphilis CW, Schultz EB Yuceer C, 2011. Poplar maintains zinc homeostasis with heavy metal genes *HMA4* and *PCS1*. Journal of Experimental Botany 62: 3737-3752

Assuncao A, Da Costa Martins P, De Folter S, Vooijis R, Schat H, Aarts M, 2001. Elevated expression of metal transporter genes in three accessions of the metal hyperaccumulator *Thalspi caerulescens*. Plant, Cell, and Environment 24: 217-226

Balesaria S, Hogstrand C, 2006. Identification, cloning and characterization of a plasma membrane zinc efflux transporter, TrZnT-1, from fugu pufferfish (*Takifugu rubripes*). Biochemical Journal 394: 485-493

Becher M, Talke IN, Krall L, Kramer U, 2004. Cross-species microarray transcript profiling reveals high constitutive expression of metal homeostasis genes in shoots of the zinc hyperaccumulator *Arabidopsis halleri*. Plant Journal 37: 251-268

Bernard C, Roosens N, Czernic P, Lebrun M, Verbruggen N, 2004. A novel CPx-ATPase from the cadmium hyperaccumulator *Thlaspi caerulescens*. FEBS Letters 569: 140-148

Blaudez D, Kohler A, Martin F, Sanders D, Chalot M, 2003. Poplar metal tolerance protein 1 confers zinc tolerance and is an oligomeric vacuolar zinc transporter with an essential leucine zipper motif. Plant Cell 15: 2911-2928

Chen WR, Feng Y and Chao YE, 2008. Genomic analysis and expression pattern of *OsZIP1, OsZIP3,* and *OsZIP4* in two rice *(Oryza sativa L.)* genotypes with differnt zinc efficiency. Russian Journal of Plant Physiology 55: 400-409

Chiang HC, Lo JC, Yeh KC, 2006. Genes associated with heavy metal tolerance and accumulation in Zn/Cd hyperaccumulator *Arabidopsis halleri*: a genomic survey with cDNA microarray. Environmental Science and Technology 40: 6792-6798

Clemens S, Kim EJ, Neumann D, Schroeder JI, 1999. Tolerance to toxic metals by a gene family of phytochelatin synthases from plants and yeast. EMBO Journal 18: 3325-3333

Clough SJ, 2005. Floral dip: *Agrobacterium*-mediated germ line transformation. Methods in Molecular Biology 286: 91-102

de Guimaraes MA, Gustin JL, Salt DE, 2009. Reciprocal grafting separates the roles of the root and shoot in zinc hyperaccumulation in *Thlaspi caerulescens*. New Phytologist 184: 323-329

Devergnas S, Chimienti F, Naud N, Pennequin A, Coquerel Y, Chantegrel J, Favier A, Seve M, 2004. Differential regulation of zinc efflux transporters *ZnT-1, ZnT-5* and *ZnT-7* gene expression by zinc levels: a real-time RT-PCR study. Biochemical Pharmacology 68: 699-709

Di Baccio D, Kopriva S, Sebastiani L, Rennenberg H, 2005. Does glutathione metabolism have a role in the defence of poplar against zinc excess? New Phytologist 167: 73-80

Edgar RC, 2004. MUSCLE: multiple sequence lignbment with high accuracy and high throughput. Nucleic Acids Research 32: 1795-1797

Eng BH, Guerinot ML, Eide D, Saier MH, Jr., 1998. Sequence analyses and phylogenetic characterization of the ZIP family of metal ion transport proteins. Journal of Membrane Biology 166: 1-7

Gaither LA, Eide DJ, 2001. Eukaryotic zinc transporters and their regulation. Biometals 14: 251-270

Grispen VMJ, Hakvoort HWJ, Bliek T, Verkleij JAC, Schat H, 2011. Combined expression of the *Arabidopsis* metallothionein MT2b and the heavy metal transporting ATPase HMA4 enhances cadmium tolerance and the root to shoot translocation of cadmium and zinc in tobacco. Envionmental and Experimental Botany 72: 71-76

Grotz N, Fox T, Connolly E, Park W, Guerinot ML, Eide D, 1998. Identification of a family of zinc transporter genes from *Arabidopsis* that respond to zinc deficiency. Proceedings of the National Academy of Sciences 95: 7220-7224

Guerinot ML, 2000. The *ZIP* family of metal transporters. Biochimica et Biophysica Acta 1465: 190-198

Hammond JP, Bowen HC, White PJ, Mills V, Pyke KA, Baker AJ, Whiting SN, May ST, Broadley MR, 2006. A comparison of the *Thlaspi caerulescens* and *Thlaspi arvense* shoot transcriptomes. New Phytologist 170: 239-260

Hartwig A, Asmuss M, Ehleben I, Herzer U, Kostelac D, Pelzer A, Schwerdtle T, Burkle A, 2002. Interference by toxic metal ions with DNA repair processes and cell cycle control: molecular mechanisms. Environmental Health Perspectives 110 797-799

Infante C, Matsuoka MP, Asensio E, Canavate JP, Reith M, Manchado M, 2008. Selection of housekeeping genes for gene expression studies in larvae from flatfish using real-time PCR. BMC Molecular Biology 9: 28

Kawachi M, Kobae Y, Mori H, Tomioka R, Lee Y, Maeshima M, 2009. A mutant strain *Arabidopsis thaliana* that lacks vacuolar membrane zinc transporter MTP1 revealed the latent tolerance to excessive zinc. Plant Cell Physiology 50: 1156-1170

Kohler A, Blaudez D, Chalot M, Martin F, 2004. Cloning and expression of multiple metallothioneins from hybrid poplar. New Phytologist 164: 83-93

Kupper H, Kochian LV, 2010. Transcriptional regulation of metal transport genes and mineral nutrition during acclimatization to cadmium and zinc in the Cd/Zn hyperaccumulator, *Thlaspi caerulescens* (Ganges population). New Phytologist 185: 114-129

Kupper H, Seib LO, Sivaguru M, Hoekenga OA, Kochian LV, 2007. A method for cellular localization of gene expression via quantitative in situ hybridization in plants. Plant Journal 50: 159-175

Lee J, Bae H, Jeong J, Lee JY, Yang YY, Hwang I, Martinoia E, Lee Y, 2003. Functional expression of a bacterial heavy metal transporter in *Arabidopsis* enhances resistance to and decreases uptake of heavy metals. Plant Physiology 133: 589-596

Lombi E, Tearall KL, Howarth JR, Zhao FJ, Hawkesford MJ, McGrath SP, 2002. Influence of iron status on cadmium and zinc uptake by different ecotypes of the hyperaccumulator *Thlaspi caerulescens*. Plant Physiology 128: 1359-1367

Long XX, Yang XE, Ni WZ, Ye ZQ, He ZL, Calvert DV, Stoffella JP, 2003. Assessing zinc thresholds for phytotoxicity and potential dietary toxicity in selected vegetable crops. Communications in Soil Science and Plant Analysis 24: 1412-1434

Lopez-Millan AF, Ellis DR, Grusak MA, 2004. Identification and characterization of several new members of the *ZIP* family of metal ion transporters in *Medicago truncatula*. Plant Molecular Biology 54: 583-596

Mäser P, Thomine S, Schroeder JI, Ward JM, Hirschi K, Sze H, Talke IN, Amtmann A, Maathuis FJM, Sanders D, Harper JF, Tchieu J, Gribskov M, Persans MW, Salt DE, Kim SA, Guerinot ML, 2001. Phylogenetic relationships within cation transporter families of *Arabidopsis*. Plant Physiology 126: 1646-1667

Michaelis A, Takehisa RS, Reiger R, Aurich O, 1986. Ammonium chloride and zinc sulfate pretreatments reduce the yield of chromatid aberrations induced by TEM and maleic hydrazide in *Vicia faba*. Mutation Research 173: 187-191

Migeon A, Blaudez D, Wilkins O, Montanini B, Campbell MM, Richaud P, Thomine S, Chalot M, 2010. Genome-wide analysis of plant metal transporters, with an emphasis on poplar. Cellular and Molecular Life Sciences 67: 3763-3784

Mills RF, Krijger GC, Baccarini PJ, Hall JL, Williams LE, 2003. Functional expression of AtHMA4, a P1B-type ATPase of the Zn/Co/Cd/Pb subclass. Plant Journal 35: 164-176

Milner MJ, Kochian LV, 2008. Investigating heavy-metal hyperaccumulation using *Thlaspi caerulescens* as a model system. Annals of Botany 102: 3-13

Moreau S, Thomson RM, Kaiser BN, Trevaskis B, Guerinot ML, Udvardi MK, Puppo A, Day DA, 2002. *GmZIP1* encodes a symbiosis-specific zinc transporter in soybean. Journal of Biological Chemistry 277: 4738-4746

Papoyan A, Kochian LV, 2004. Identification of *Thlaspi caerulescens* genes that may be involved in heavy metal hyperaccumulation and tolerance. Characterization of a novel heavy metal transporting ATPase. Plant Physiology 136: 3814-3823

Pence NS, Larsen PB, Ebbs SD, Letham DL, Lasat MM, Garvin DF, Eide D, Kochian LV, 2000. The molecular physiology of heavy metal transport in the Zn/Cd hyperaccumulator *Thlaspi caerulescens*. Proceedings of the National Academy of Sciences 97: 4956-4960

Ramesh SA, Choimes S, Schachtman DP, 2004. Over-expression of an *Arabidopsis* zinc transporter in *Hordeum vulgare* increases short-term zinc uptake after zinc deprivation and seed zinc content. Plant Molecular Biology 54: 373-385

Rood SB, Braatne JH, Hughes FM, 2003. Ecophysiology of riparian cottonwoods: stream flow dependency, water relations and restoration. Tree Physiology 23: 1113-1124

Stamatakis A, 2006. RAxML-VI-HPC: maximum likelihood-based phylogenetic analyses with thousands of taxa and mixed models. Bioinformatics 22: 2688-2690

Stamatakis A, Ludwig T, Meier H, 2005. RAxML-III: a fast program for maximum likelihood-based inference of large phylogenetic trees. Bioinformatics 21: 456-463

Tuskan GA, Difazio S, Jansson S, Bohlmann J, Grigoriev I, Hellsten U, Putnam N, Ralph S, Rombauts S, Salamov A, Schein J, Sterck L, Aerts A, Bhalerao RR, Bhalerao RP, Blaudez D, Boerjan W, Brun A, Brunner A, Busov V, Campbell M, Carlson J, Chalot M, Chapman J, Chen GL, Cooper D, Coutinho PM, Couturier J, Covert S, Cronk Q, Cunningham R, Davis J, Degroeve S, Dejardin A, Depamphilis C, Detter J, Dirks B, Dubchak I, Duplessis S, Ehlting J, Ellis B, Gendler K, Goodstein D, Gribskov M, Grimwood J, Groover A, Gunter L, Hamberger B, Heinze B, Helariutta Y, Henrissat B, Holligan D, Holt R, Huang W, Islam-Faridi N, Jones S, Jones-Rhoades M, Jorgensen R, Joshi C, Kangasjarvi J, Karlsson J, Kelleher C, Kirkpatrick R, Kirst M, Kohler A, Kalluri U, Larimer F, Leebens-Mack J, Leple JC, Locascio P, Lou Y, Lucas S, Martin F, Montanini B, Napoli C, Nelson DR, Nelson C, Nieminen K, Nilsson O, Pereda V, Peter G, Philippe R, Pilate G, Poliakov A, Razumovskaya J, Richardson P, Rinaldi C, Ritland K, Rouze P, Ryaboy D, Schmutz J, Schrader J, Segerman B, Shin H, Siddiqui A, Sterky F, Terry A, Tsai CJ, Uberbacher E, Unneberg P, Vahala J, Wall K, Wessler S, Yang G, Yin T, Douglas C, Marra M, Sandberg G, Van de Peer Y, Rokhsar D, 2006. The genome of black cottonwood, *Populus trichocarpa* (Torr. & Gray). Science 313: 1596-1604

Tusnady GE, Simon I, 1998. Principles governing amino acid composition of integral membrane proteins: application to topology prediction. Journal of Molecular Biology 283: 489-506

van de Mortel JE, Almar Villanueva L, Schat H, Kwekkeboom J, Coughlan S, Moerland PD, Ver Loren van Themaat E, Koornneef M, Aarts MG, 2006. Large expression differences in genes for iron and zinc homeostasis, stress response, and lignin biosynthesis distinguish roots of Arabidopsis thaliana and the related metal hyperaccumulator *Thlaspi caerulescens*. Plant Physiology 142: 1127-1147

Wan CY, Wilkins TA, 1994. A modified hot borate method significantly enhances the yield of high-quality RNA from cotton (*Gossypium hirsutum* L.). Analytical Biochemistry 233: 7-12

Wu J, Zhao FJ, Ghandilyan A, Brabara L, Guzman MO, Schat H, Wang X, Aarts M, 2009. Identification and functional analysis of two ZIP metal transporters of the hyperaccumulator *Thlaspi caerulescens*. Plant and Soil 325: 79-95

Yang X, Huang J, Jiang Y, Zhang HS, 2009. Cloning and functional identification of two members of the *ZIP* (Zrt, Irt-like protein) gene family in rice (*Oryza sativa* L.). Molecular Biology Reports 36: 281-287

Appendix S1. Primer list for poplar gene expression analyses via qPCR and gene isolation and promoter cloning via RT-PCR.

Gene Name	Poplar ID	PrimerDirection	Sequence
PtZIP1.2	POPTR_0008s08260.1	Forward	GGCTCTGTCTGAAATGGTTCG TCG
PtZIP1.2	POPTR_0008s08260.1	Reverse	GGCAATTCCCAGTGGGGTTGT CAGGG
PtZNT1	POPTR_0018s05190.1	Forward	CCGAACAGCCCAAGAGCAT
PtZNT1	POPTR_0018s05190.1	Reverse	CGGCCGACAGAGAATCTAAGA
PtZNT1	POPTR_0018s05190.1	Taqman Probe	6FAM AGCCGCTGAAGGC
UBQ (Taqman)	POPTR_0001s13770.1	Forward	CTTTGCCGGAAAGCAGTTG
UBQ (Taqman)	POPTR_0001s13770.1	Reverse	CGGAGACGGAGGACAAGGT
UBQ (Taqman)	POPTR_0001s13770.1	Taqman Probe	6FAMCGCACCCTAGCAGAC
UBQ (Sybr-Green)	POPTR_0001s13770.1	Forward	CGATAATGTGAAGGCCAAAA TTCAG
GUS		Forward	GTTGGGCAGGCCAGCGTATCG TGC
GUS		Reverse	CATCACGCAGTTCAACGCTGA CATC

PromoterName	Primer Direction	Primer Type	Sequence
Pro$_{PtZNT1}$:GUS	Forward	Isolation	GGCTATTTGGTAAGCTATGTC
Pro$_{PtZNT1}$:GUS	Reverse	Isolation	GGTGATTTAGAGATTGCTTC
Pro$_{PtZNT1}$:GUS	Forward	Restriction (*Sph1*)	GCGCATGCCTATTTGGTAAGC
Pro$_{PtZNT1}$:GUS	Reverse	Restriction (*Nco1*)	GGCTGCAGCCATGGTGATTTAG AGATTGC
Pro$_{TcZNT1}$:GUS	Forward	GenomicWalking (*DraI* library)	GGAACGAGGTTGCTGGTGGTGG
Pro$_{TcZNT1}$:GUS	Forward	GenomicWalking (*PvuII*Library)	CCCAAGGTGGATATATGACT AACGTCGGCG
Pro$_{TcZNT1}$:GUS	Forward	Isolation	CCCGTGGGAGAAGAAGCCATTG TCTGC
Pro$_{TcZNT1}$:GUS	Forward	Isolation	GCGCTCCCGGCCGCCATGGCGG CCGCGGG
Pro$_{TcZNT1}$:GUS	Forward	Restriction (*HindIII*)	CCAAGCTTGCGTGGGTTTA TGTGGAGG
Pro$_{TcZNT1}$:GUS	Forward	Restriction (*BamHI*)	GGAAGCTTGGATCCTGTCTG CAAAATGGACTC

Appendix S2. Gene names, accession numbers, and predicted transmembrane helices for PtZNT1 genes in a phylogenetic tree of ZNT1-like genes (Fig. 1a) and ZIP-like genes (Fig. 1b). The Section column indicates which tree (i.e., Fig. 1a, Fig. 1b, or both) the gene appears in.

Gene ID	Accession	Section	Transmembrane Helices
PtZIP4.4	POPTR 0006s00860.1	AB	9
PtZIP4.1	POPTR 0006s00870.1	AB	3
PtZIP (1)	POPTR 0006s00840.1	AB	8
PtZIP (2)	POPTR 0001s16050.1	AB	4
PtZIP1.1	POPTR 0010s18050.1	AB	8
PtZIP1.2	POPTR 0008s08260.1	AB	9
PtZIP6.4	POPTR 0015s15750.1	AB	8
PtZIP (3)	POPTR 0015s15730.1	AB	8
PtZIP7.2	POPTR 0010s14430.1	AB	9
PtZIP (4)	POPTR 0010s14550.1	AB	8
PtZIP6.3	POPTR 0001s28620.1	AB	8
PtZIP6.2	POPTR 0009s07810.1	AB	8
PtZIP (5)	POPTR 0018s05190.1	AB	8
MeZIP	Cassava29071.valid.m1	A	8
RcZIP	29794.m003320	A	8
CpZIP	Evm.model.supercontig 7.170	A	8
MgZIP	Mgf004428	A	8
GmZIP (1)	Glyma04g054101	A	4
MtZIP (1)	Medtr3g139990.1	A	8
MtZIP (2)	Medtr1g020230.1	A	8
GmZIP (2)	Glyma14g10840.1	A	4
GmZIP (3)	Glyma17g34660.1	A	8
AtIRT3	At1g60960.1	AB	8
AlZNT (1)	315258	A	8
TcZNT1	AF133267	AB	8
TjZNT1	AB206397.1	A	8
AlZIP (2)	888393	A	8
AtZIP4	At1g10970.1	AB	8
AlZIP (3)	353523	A	8
AtZIP9	At4g33020.1	AB	8
VvZIP	GSVIVT00032208001	A	8
CsZIP	Cucsa.395110.1	A	8
OsZIP10	Os06g37010.2	AB	8
OsZIP3	Os04g52310.1	AB	8
OsZIP4	Os08g10630.1	AB	9
OsZIP7	Os05g10940.1	AB	8
SbZIP10	Sb10g022390.1	AB	4
SbZIP3	Sb06g028270.1	AB	8
SbZIP4	Sb07g006060.1	AB	4
SbZIP7	Sb09g006150.1	AB	8
AtZIP1	At3g12750.1	B	8
AtZIP3	At2g32270.1	B	9
AtZIP7	At2g04032.1	B	8
AtZIP5	At1g05300.1	B	9
AtIRT1	At4g19690.2	B	9
AtZIP12	At5g62160.1	B	9
AtZIP10	At1g31260.1	B	9
AtIRT2	At4g19680.2	B	9
AtZIP8	At5g45105.2	B	7
AtZIP6	At2g30080.1	B	7

Appendix S3. Transcriptional ratio [log10(target gene/UBQ)] averages and variances across three metal treatments at 24h and 48h for each tissue.

Tissue	Gene Name	Day	Metal Treatment	N	Average of Ratios	Vaiance of Ratios
Leaf	PtZNT1	1	1µM	9	2.51	0.21
Leaf	PtZNT1	1	10µM	9	2.66	0.42
Leaf	PtZNT1	1	1mM	9	3.36	0.63
Leaf	PtZNT1	2	1µM	9	2.94	0.53
Leaf	PtZNT1	2	10µM	9	2.56	0.46
Leaf	PtZNT1	2	1mM	9	2.77	0.39
Root	PtZNT1	1	1µM	9	1.62	1.10
Root	PtZNT1	1	10µM	9	2.22	0.81
Root	PtZNT1	1	1mM	9	0.92	0.38
Root	PtZNT1	2	1µM	9	2.68	0.45
Root	PtZNT1	2	10µM	9	1.57	0.33
Root	PtZNT1	2	1mM	9	0.97	0.46
Stem	PtZNT1	1	1µM	9	2.27	0.72
Stem	PtZNT1	1	10µM	9	3.02	0.75
Stem	PtZNT1	1	1mM	9	1.59	0.42
Stem	PtZNT1	2	1µM	9	1.86	0.65
Stem	PtZNT1	2	10µM	9	2.64	0.52
Stem	PtZNT1	2	1mM	9	2.35	0.39
Root	PtZIP1	1	1µM	9	21.34	906.94
Root	PtZIP1	1	10µM	9	3.09	13.12
Root	PtZIP1	1	1mM	9	1.96	3.50
Root	PtZIP1	2	1µM	9	12.72	147.75
Root	PtZIP1	2	10µM	9	3.57	28.89
Root	PtZIP1	2	1mM	9	41.61	1577.45
Stem	PtZIP1	1	1µM	9	2.68	1.91
Stem	PtZIP1	1	10µM	9	9.76	129.26
Stem	PtZIP1	1	1mM	9	4.82	67.54
Stem	PtZIP1	2	1µM	9	27.55	453.31
Stem	PtZIP1	2	10µM	9	6.51	8.55
Stem	PtZIP1	2	10µM	9	6.51	8.55

Appendix S4. Transcriptional ratio (*GUS*/*UBQ*) averages from leaf and root tissues of *Pro*$_{PtZNT1}$*:GUS* and *Pro*$_{TcZNT1}$*:GUS* constructs.

Tissue	Construct	N	Ratio Average	Ratio ariance
Leaf	Wild-type	3	0.00	0.00
Leaf	*Pro*$_{PtZNT1}$*:GUS*	3	0.31	0.00
Leaf	*Pro*$_{PtZNT1}$*:GUS*	3	0.02	0.00
Leaf	*Pro*$_{PtZNT1}$*:GUS*	3	0.03	0.00
Leaf	*Pro*$_{TcZNT1}$*:GUS*	3	0.00	0.00
Leaf	*Pro*$_{TcZNT1}$*:GUS*	3	0.41	0.01
Leaf	*Pro*$_{TcZNT1}$*:GUS*	3	0.62	0.00
Root	*Pro*$_{PtZNT1}$*:GUS*	3	0.10	0.01
Root	*Pro*$_{PtZNT1}$*:GUS*	3	0.08	0.00
Root	*Pro*$_{PtZNT1}$*:GUS*	3	0.36	0.06
Root	*Pro*$_{TcZNT1}$*:GUS*	3	0.82	0.08
Root	*Pro*$_{TcZNT1}$*:GUS*	3	0.21	0.00
Root	*Pro*$_{TcZNT1}$*:GUS*	3	0.35	0.00